Guide to Canine and Feline Electrocardiography

Edited by Ruth Willis, Pedro Oliveira and Antonia Mavropoulou

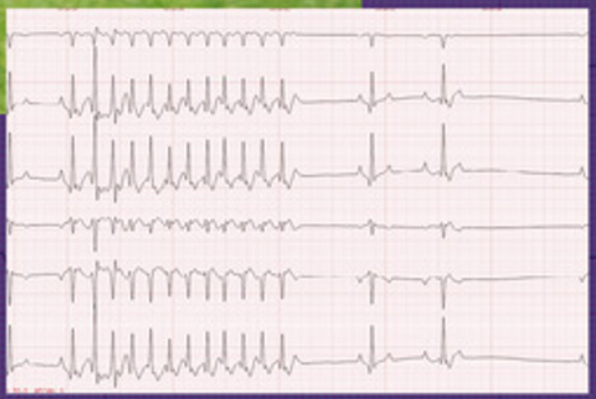

with website

WILEY Blackwell

Guide to Canine and Feline Electrocardiography

Guide to Canine and Feline Electrocardiography

Ruth Willis

BVM&S DVC MRCVS
RCVS Recognised Specialist in Veterinary Cardiology
Holter Monitoring Service
Dick White Referrals
Newmarket
Cambridgeshire, UK
and
Honorary Associate Professor
University of Nottingham
Nottingham, UK

Pedro Oliveira

DVM, Diplomate ECVIM-CA (Cardiology), MRCVS
RCVS Recognised Specialist in Veterinary Cardiology
Davies Veterinary Specialists
Higham Gobion
Hertfordshire, UK

Antonia Mavropoulou

DVM, PhD, Diplomate ECVIM-CA (Cardiology), MRCVS
RCVS Recognised Specialist in Veterinary Cardiology
Davies Veterinary Specialists
Higham Gobion
Hertfordshire, UK

WILEY Blackwell

This edition first published 2018

Registered Offices
John Wiley & Sons, Inc., 111 River Street, Hoboken, NJ 07030, USA
John Wiley & Sons Ltd, The Atrium, Southern Gate, Chichester, West Sussex, PO19 8SQ, UK

Editorial Office
9600 Garsington Road, Oxford, OX4 2DQ, UK

For details of our global editorial offices, customer services, and more information about Wiley products visit us at www.wiley.com.

Wiley also publishes its books in a variety of electronic formats and by print-on-demand. Some content that appears in standard print versions of this book may not be available in other formats.

Library of Congress Cataloging-in-Publication Data

Names: Willis, Ruth, 1973– author. | Oliveira, Pedro, 1980– author. | Mavropoulou, Antonia, author.
Title: Guide to canine and feline electrocardiography / Ruth Willis, Pedro Oliveira, Antonia Mavropoulou.
Description: Hoboken, NJ : John Wiley & Sons, Inc., [2018] | Includes bibliographical references and index. |
Identifiers: LCCN 2018007638 (print) | LCCN 2018009442 (ebook) | ISBN 9781119254300 (pdf) | ISBN 9781119254317 (epub) | ISBN 9781119253846 (cloth)
Subjects: | MESH: Arrhythmias, Cardiac–veterinary | Electrocardiography–veterinary | Dog Diseases–diagnosis | Cat Diseases–diagnosis
Classification: LCC SF772.58 (ebook) | LCC SF772.58 (print) | NLM SF 992.C37 | DDC 636.089/61207543–dc23
LC record available at https://lccn.loc.gov/2018007638

Cover Design: Wiley
Cover Images: (Dog photo) Steve Magennis, Working Dogs in Action photography; (ECG report) Pedro Oliveira

Set in 10/12pt Warnock by SPi Global, Pondicherry, India

10 9 8 7 6 5 4 3 2 1

Contents

List of Contributors

Erin L. Anderson
VMD, MSc, DACVIM (cardiology)
Associate Cardiologist
Pittsburgh Veterinary Specialty and Emergency Center
Pittsburgh, USA

Domingo Casamian-Sorrosal
DVM, Cert SAM, DVC, Diplomate ECVIM-CA, MRCVS
RCVS Diplomate and Recognised Specialist in Veterinary Cardiology
ECVIM Diplomate and Specialist in Small Animal Internal Medicine
Southfields Vet Specialists
Laindon
Essex, UK

Louise Clark
BVMS, Cert VA, Diplomate ECVAA, MSc (Clinical Management of Pain), MRCVS
Davies Veterinary Specialists
Higham Gobion
Hertfordshire, UK

Frances Downing
BVSc, MSc, Diplomate ECVAA, MRCVS
Davies Veterinary Specialists
Higham Gobion
Hertfordshire, UK

Martin Lowe
BSc, MB, BS, PhD, FRCP
Cardiology Consultant
BARTS Heart Centre
London, UK

Antonia Mavropoulou
DVM, PhD, Diplomate ECVIM-CA (Cardiology), MRCVS
RCVS Recognised Specialist in Veterinary Cardiology
Davies Veterinary Specialists
Higham Gobion
Hertfordshire, UK

Pedro Oliveira
DVM, Diplomate ECVIM-CA (Cardiology), MRCVS
RCVS Recognised Specialist in Veterinary Cardiology
Davies Veterinary Specialists
Higham Gobion
Hertfordshire, UK

Romain Pariaut
DVM, Diplomate ACVIM and ECVIM-CA (Cardiology)
Associate Professor of Cardiology, Section Chief of Cardiology
Cornell University, College of Veterinary Medicine, Department of Clinical Sciences
Ithaca, USA

Thibault Ribas
DVM, Diplomate ECVIM-CA (Cardiology)
Azurvet
Cagnes-Sur-Mer, France

Joel Freitas da Silva
DVM, Diplomate ECVIM-CA (Cardiology), MRVC
RCVS Recognised Specialist in Cardiology
North Downs Specialist Referrals
Bletchingley
Surrey, UK

Simon Swift
MA, VetMB, CertSAC, DipECVIM-CA (Cardiology), MRCVS
Clinical Associate Professor – Cardiology
Department of Small Animal Clinical Sciences
University of Florida
Gainesville, USA

Marin Torti
DVM, PhD
Clinic for Internal Diseases, Faculty of Veterinary Medicine, University of Zagreb
Zagreb, Croatia

Gerhard Wess
DVM, Dr. med. vet., Dr. habil., Diplomate ACVIM (Cardiology), Diplomate ECVIM-CA (Internal Medicine and Cardiology)
Clinic for Small Animal Medicine, Ludwig-Maximilian University
Munich, Germany

Ruth Willis
BVM&S, DVC, MRCVS
RCVS Recognised Specialist in Veterinary Cardiology
Holter Monitoring Service
Dick White Referrals
Newmarket
Cambridgeshire, UK

Jon Wray
BVSc, CertVC, Diplomate ECVIM-CA (Internal Medicine), MRCVS
Holter Monitoring Service
Dick White Referrals
Newmarket
Cambridgeshire, UK

Preface

To many veterinary students, veterinarians and veterinary nurses, electrocardiography (ECG) can seem like a daunting challenge and somewhat of a mystery. Arrhythmias can be life threatening and anti-arrhythmic drugs may have the potential to be pro-arrhythmic, factors which often intimidate clinicians and can instill a fear of possibly harming rather than helping a patient. However, for those who master this challenge, they find ECG thoroughly rewarding as it is one of the more logical fields in veterinary medicine and it appeals to the puzzle solver in us.

The authors of this *Guide to Canine and Feline Electrocardiography* have undertaken the challenge of bringing together their expertise in understanding the pathophysiology, but also diagnosing and managing arrhythmias in an outstanding, extensive review of cardiac ECG.

The reader is taken systematically through the basics of ECG generation: the required equipment for ECG acquisition, detailed explanation of the mechanisms underlying arrhythmias as well the evaluation of the arrhythmia substrate. The book provides advanced, up-to-date description of all important arrhythmias encountered in dogs and cats, highlighting both the main characteristics and breed-specific differences and in-depth therapeutic considerations. The authors have taken a highly visual approach, where all phenomena described are illustrated with original colour figures and beautiful ECG traces. Examples of normal ECG recordings, practice electrocardiograms and a diagnostic approach to real-life electrocardiograms of many clinically important arrhythmias will help the reader to feel comfortable and confident to interpret even the most complex arrhythmias. Valuable review questions, self-assessment sections as well as recommended reading are also built-in, and a comprehensive list of references are provided at the end of each chapter.

This book is a first of its kind in veterinary medicine as it also includes chapters on arrhythmia interpretation using long-term ambulatory ECG (Holter or event recorder) monitoring; provides insight into interpretation of heart rate variability parameters and detailed description of pacemaker therapies, including surgical implantation techniques and programming instructions; and delivers valuable information on abnormal ECGs encountered in veterinary patients under anesthesia.

For those interested in advanced, interventional arrhythmia therapies, a large chapter is dedicated to cutting-edge techniques of radiofrequency ablation, and the reader is presented with practical tips on how to set up an electrophysiology laboratory and taught the step-by-step approach on interpretation of intracardiac electrograms.

For all these reasons, this comprehensive veterinary ECG book is worth the highest merit, and undoubtedly deserves to be in every personal library of veterinary students, residents, veterinarians and veterinary nurses.

Anna Gelzer, Dr.med.vet. PhD
LDACVIM & ECVIM-CA-Cardiology
Associate Professor of Cardiology
School of Veterinary Medicine
University of Pennsylvania, USA

Acknowledgements

The decision to write a book was relatively straightforward but then, as the enormity of the task became apparent, we were incredibly fortunate to have so many people willing to help us achieve our objective.

Firstly I would like to remind my family – Greg, Sophie and Josh – that you are, and always will be, the most important part of my life. Thank you is such a small phrase to encompass the sacrifices you have all made over the last two years, and I could not have completed this project without your support, patience and encouragement.

Secondly I would like to thank Pedro and Antonia who have patiently filtered my ideas. You have both been an invaluable source of knowledge and reassurance on this journey, and your attention to detail is reflected in the quality of this book.

Also thanks to all the chapter authors for giving us your precious time and expertise to improve the quality and breadth of this book. Thanks too to numerous colleagues who have assisted us by supplying figures and providing constructive criticism and encouragement along the way.

A special thanks is due to Paul Wotton for his mentorship throughout my career and to the team at Dick White Referrals, who ask good questions and are constantly striving to improve the care we provide for our patients. I am privileged to have such inspiring colleagues.

I would like to thank Wiley for believing in us, their commitment to this project and the hard work of all involved.

Last but not least, thanks to my parents Helen and Ray. You are the people who taught me to work hard and persevere. Thanks also to our extended family and all our friends – I am immensely grateful for the support, company and humour you bring to my life.

December 2017 **Ruth Willis**

To my family, friends and colleagues for all their support.

Pedro Oliveira

To my family, friends and mentors for their love, support and encouragement.

Antonia Mavropoulou

About the Companion Website

Don't forget to visit the companion website for this book:

www.wiley.com/go/willis/electrocardiography

There you will find valuable material designed to enhance your learning, including:

- Self-assessment questions
- Figures from the book
- Appendices.

Scan this QR code to visit the companion website:

1

Anatomy of the Conduction System

Pedro Oliveira

Introduction

The heart possesses a specialised conduction system that is responsible for generating and transmitting electrical stimuli to the whole heart in a specific and ordered fashion. It is composed of the sinoatrial node (SA), internodal and inter-atrial pathways, atrioventricular junction, bundle branches and Purkinje fibres (Figure 1.1). The SA contains specialised 'pacemaker' cells that have the ability to spontaneously depolarise, generating electrical impulses. The remainder of the conduction system is composed mainly of cells organised in bundles that allow conduction of the electrical stimuli. These structures are present in the walls of the heart and are interwoven with the myocardial tissue itself. It is not possible to distinguish them from the rest of the myocardium (working myocardium) with the naked eye, only with certain stains under the microscope.

The anatomy of these structures is presented in this chapter. To avoid confusion, the use of human anatomical terminology is avoided, and terminology commonly used in veterinary medicine for quadruped patients is preferred. Given the different orientation of the heart within the chest of dogs and cats in comparison to humans, the following terms are used: cranial instead of anterior; caudal instead of posterior; dorsal instead of superior; and ventral instead of inferior. However, since some terms are so widespread in veterinary literature (e.g. left anterior or posterior fascicles), it is difficult to avoid the use of such terms even though they are not entirely appropriate.

Sinoatrial Node

Anatomy

The SA, also known as the sinus node, is found in the wall of the right atrium at its junction with the cranial vena cava in the upper portion of the terminal groove (sulcus terminalis) (Figure 1.1).

In dogs, it lies less than 1 mm beneath the epicardium and occupies almost the entire thickness of the atrial wall from epicardium to endocardium.[1] The total size of the canine node was described as being approximately 5 mm^3 with an oblong shape, although with significant variation observed amongst individuals.[1,2] Other reports suggest a more extensive location of up to 3–4 cm between both venae cavae.[3,4]

In cats, according to one study including five male and five female domestic shorthair cats, the SA node was located 0.06–0.11 mm beneath the epicardium with an almost triangular shape.[5] In males the reported size was $2.78 \times 2.80 \times 0.54$ mm, and in females it was $2.75 \times 2.64 \times 0.45$ mm.[5] A different study involving 12 cats produced different results.[6] A reconstruction of the SA node based on histological and electrophysiological data was performed in five of these cats, revealing an ellipsoid shape with a total area of 10.5 ± 0.76 mm^2, a maximum length of 7.4 ± 0.74 mm, a maximal width of 2.2 ± 0.10 mm and a thickness of 0.41 ± 0.060 mm.[6]

Histology

Histologically, the SA is composed of specialised muscle fibres arranged in a network.[7] Many small bundles are present with irregular courses interspersed with connective tissue accompanied by capillary vessels and nerve cells. The surface of the SA is covered by epicardium, and the remaining areas are surrounded by atrial muscle. Each nodal fibre shows a smooth transition to ordinary atrial muscle fibres at the periphery of the SA.

Three different types of cells are present: normal working myocardial cells, transitional cells and P (pacemaker) cells.

The P cells are responsible for the ability of the SA to spontaneously generate electrical stimuli. They represent approximately 50% of the cells in the SA and are also present in other areas of the conduction system

Guide to Canine and Feline Electrocardiography, First Edition. Ruth Willis, Pedro Oliveira and Antonia Mavropoulou.

Companion website: www.wiley.com/go/willis/electrocardiography

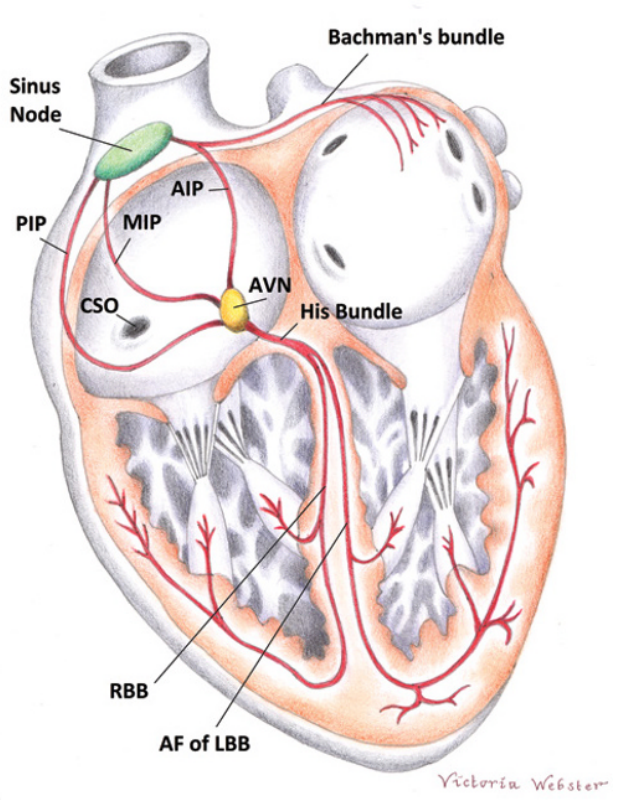

Figure 1.1 Cardiac conduction system. The sinoatrial node, also known as the sinus node, is found in the wall of the right atrium at its junction with the cranial vena cava in the upper portion of the terminal groove (sulcus terminalis). It is connected to the atrioventricular node (AVN) located on the floor of the right atrium via the anterior (AIP), middle (MIP) and posterior (PIP) internodal pathways. Connections also exist between the right and left atria, of which Bachmann's bundle and the inferior interatrial pathway (not illustrated) are the most important. Bachmann's bundle runs in the upper portion of the atrial septum towards the left auricle. The inferior interatrial pathway is composed of fibres that are continuous with the right atrial myocardium at the level of the ostium of the coronary sinus (CSO) and with the left atrial myocardium from which they separate approximately 20–30 mm from the CSO. The AVN is continued by the Bundle of His that penetrates the fibrous skeleton of the heart and ramifies into the right (RBB) and left (LBB) bundle branches. The LBB is composed of anterior (AF) and posterior ramifications (not illustrated). The bundle branch subdivisions give rise to numerous small branches that spread all over the subendocardium of both ventricles, forming the Purkinje network that connects the conduction system to the working myocardium.

(e.g. atrioventricular node [AVN]) in fewer numbers. They are organised in small groups of approximately five cells surrounded by connective tissue that function as a unit.

The transitional cells are also present in other parts of the conduction system (e.g. internodal tracts and the atrioventricular junction) and seem to provide a link between the specialised cells and the normal working myocardium.

Sinoatrial Exit Pathways

The existence of discrete exit sites has been described at the cranial and caudal ends of the canine sinus node.[8] Ablation of these sites resulted in sinoatrial block, suggesting that the SA was not anatomically continuous with the atrial myocardium.[8,9] It was suggested that vessels and connective tissue around the SA tissue were responsible for anatomical and physiological blocks on both sides of the node with the exception of the exit sites.[9] These findings, together with the reports of a length of up to 3–4 cm,[3,4] provide a plausible explanation for the occurrence of 'wandering pacemaker' in this species (see chapter 5).

Internodal Pathways

The presence of preferential pathways that connect the SA and AVN has been the subject of debate for the past century, and there is still disagreement about their existence and significance. In the dog, there is anatomical and electrophysiological evidence to support the presence of three distinct pathways in the right atrium, with cells that possess characteristics similar to those of Purkinje cells.[10] However, these pathways are not insulated from neighbouring atrial muscle and are not composed of specialised conduction cells only. This raises questions about their role, and some argue that they should not be termed *bundles* for this reason.[11] Nonetheless, surgical resection of these pathways was shown to result in a junctional rhythm in dogs, supporting their role as internodal pathways.[10]

The *anterior internodal pathway* originates in the sinus node and courses through the cranial aspect of the cranial vena cava, at which point it bifurcates into Bachman's bundle (see the 'Inter-atrial pathways' section) and a branch that courses ventrally through the cranial inter-atrial septum to join the cranial aspect of the AVN (Figure 1.1).

The *middle internodal pathway* originates in the sinus node and travels downwards cranially to the fossa ovalis towards the AVN (Figure 1.1).

The *posterior internodal pathway* originates in the sinus node, then it courses along the crista terminalis and downwards through the caudal aspect of the inter-atrial septum, past the coronary sinus (CS) ostium and joining the caudal aspect of the AVN (Figure 1.1).

Inter-atrial Pathways

At least four distinct inter-atrial electrical connections have been identified in dogs.

Bachman's bundle, or the inter-atrial band, originates close to the SA and traverses the upper portion of the inter-atrial septum towards the left auricle (Figure 1.1).

It is composed of normal atrial muscle and of specialised conducting fibres capable of rapid conduction, similar to the Purkinje fibres in the ventricles.[12]

Another connection is present ventrally via striated muscle fibres identical to atrial myocardium that surround the CS.[13] These fibres are continuous with the right atrial myocardium at the level of the CS ostium and with the left atrial myocardium from which they separate approximately 20–30 mm from the CS ostium.[14] A tract of atrial muscle that terminates blindly within the ligament or vein of Marshall (a remnant of the left cranial vena cava) has been proposed as the terminal end of this pathway in the left atrium, and the term *inferior interatrial pathway* was used to describe it.[15]

Additional connections exist at the level of the atrial septum craniodorsally, in the proximity of the fossa ovalis, and caudoventrally, possibly via the subepicardial band that connects the left atrium and cavoatrial junction ventrally.[16,17]

Bachman's bundle and the CS musculature are believed to be the major connections and the preferred pathways for conduction of electrical stimuli between the atria.[16]

The Atrioventricular Junction

The atrial and ventricular myocardium are separated by a fibrous skeleton that consists of the distinct valve annuli and intervening fibrous trigones. This structure provides attachment for the valve leaflets and the myocardium itself. As a consequence, the atrial and ventricular myocardium are electrically isolated, which is important to ensure that atrial and ventricular contractions occur in a coordinated fashion. The only point of electrical connection is provided by a specialised conduction structure that traverses the central portion of the fibrous skeleton (the *central fibrous body*), commonly described as the *atrioventricular node* or *junction* (Figures 1.1 and 1.2). It is located approximately 1 mm beneath the epicardium on the floor of the right atrium in an area known as the *triangle of Koch* (Figure 1.2).[11,18] The CS ostium limits the base of this triangle, and the apex is formed by the junction between the fibrous tendon (tendon of Todaro) and the septal leaflet of the tricuspid valve (Figure 1.2). In the dog, the AVN has an elongated shape with a concave surface facing the central fibrous body. It averages approximately 2–4 mm in length, 2 mm in width and 0.5–1 mm in thickness.[19,20] In the cat, an elongated oval shape has also been reported that is approximately 1.2–1.8 mm in length, 0.2–0.5 mm in width and 0.4–0.6 mm in thickness.[21] Male cats appear to have a larger AVN than females.[21]

The AVN can be divided into an atrionodal region formed by atrionodal bundles that converge into a proximal atrioventricular bundle, the compact node and the distal atrioventricular bundle (DAVB; Figure 1.2).[20] This division is based on histological differences between each area. The remainder of this section focuses on canine anatomy.

Atrionodal Bundles and the Proximal Atrioventricular Bundle

Three distinct atrionodal bundles have been described in the dog and are thought to be the continuation of the internodal pathways (Figure 1.2).[20,22,23] They are associated

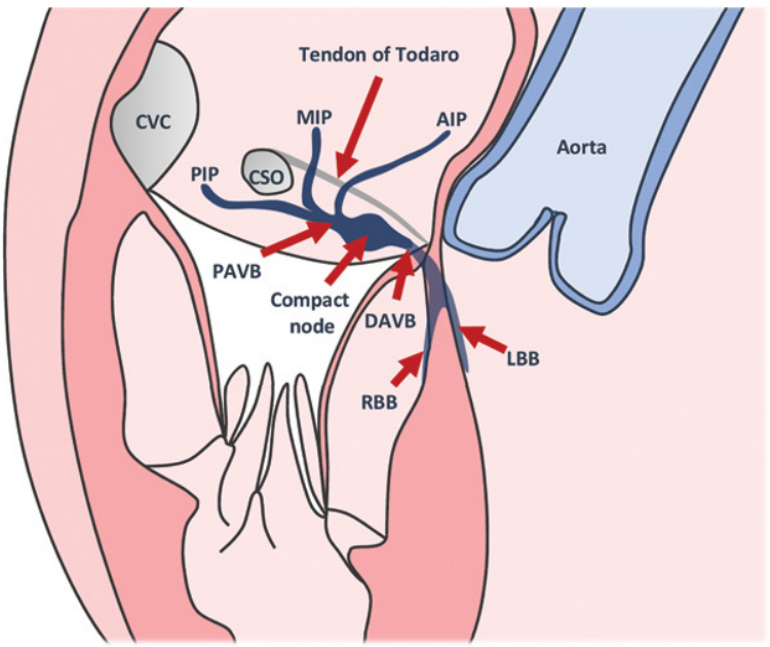

Figure 1.2 The atrioventricular junction. The atrioventricular junction may be divided into the proximal atrioventricular bundle (PAVB), the compact node and the distal atrioventricular bundle (DAVB). It is located on the floor of the right atrium in a triangular-shaped area (triangle of Koch) formed caudally by the coronary sinus ostium (CSO) and with the tendon of Todaro and the tricuspid valve rim as its lateral boundaries. The posterior (PIP), middle (MIP) and anterior (AIP) internodal pathways join the atrioventricular junction via distinct atrionodal bundles forming the PAVB. The DAVB extends from the compact node approximately 3 mm to a branching point at the cranial edge of the tricuspid septal leaflet. Here, it penetrates the septum fibrosum of the cardiac fibrous skeleton bridging the atria and ventricles. The DAVB divides into the left (LBB) and right (RBB) bundle branches at the level of the upper portion of the interventricular septum beneath the non-coronary and the right aortic leaflets. CVC, Caudal vena cava.

with epicardium of the medial right atrial wall and the crest of the ventricular septum, approximately 1 cm away from the annulus fibrosus.[20] The cells are organised into small fascicles of myofibres surrounded by collagen without connection to ordinary atrial myocardium. The myofibres run in a parallel fashion.

The *superior (dorsal) atrionodal bundle* is located beneath the epicardium of the dorsal-cranial aspect of the medial right atrial wall, closely apposed to the crest of the interventricular septum.

The *middle atrionodal bundle* is located beneath the epicardium on the dorsal-caudal aspect of the medial right atrial wall, opposed to the medial aspect of the tendon of Todaro, associated with the dorsal-medial aspect of the CS ostium.

The *lateral atrionodal bundle* input is located beneath the epicardium on the caudal-ventral aspect of the medial right atrial wall, subjacent to the lateral aspect of the CS ostium.

The presence of additional atrionodal bundles has not been proved but was suggested.[24] Remnants of bundles extending into the left atrium have been described, but further studies are necessary to determine their significance.[20]

The atrionodal bundles converge into the *proximal atrioventricular bundle* (PAVB) that is continuous with the compact node (Figure 1.2). It is located beneath the epicardium of the right atrial medial wall, cranially to the floor of the CS ostium, medially to the tendon of Todaro and approximately 1 cm away from the hinge point of the tricuspid leaflet at the annulus fibrosus. At this level, the myofibres are tightly coiled in single strands that form fascicles running in parallel.[20,25] A small number of intercalated discs are present in comparison to the atrionodal bundles. The PAVB is also characterised by numerous ganglia nestled amongst its fascicles, blood vessels and fat vacuoles and particularly prominent at the ventricular septal apposition.[25]

Compact Node

The *compact node* rests on the atrial aspect of the central fibrous body (Figure 1.2). In the dog, it is approximately 1–1.5 mm in length. From caudal to cranial, it appears initially as two half-ovals separated by the nodal artery that become fused cranially.[26] It is composed of closely interwoven fibres which frequently connect with each other within a sparse collagen framework.[7] The nodal cells are small and are arranged in a parallel fashion on the caudal aspects of the node. Cranially, they are arranged in interweaving fascicles on the left margin, and on the right the cells become larger and are arranged in a more parallel fashion. This arrangement is also seen in the proximal part of the DAVB.[11]

Distal Atrioventricular Bundle

The DAVB extends cranially from the compact node approximately 3 mm to a branching point at the cranial edge of the tricuspid septal leaflet (Figure 1.2).[20] It resides in the cranial part of the central fibrous body, where it penetrates the septum fibrosum bridging the atria and ventricles. The myocytes are larger in the DAVB, and the myofibres and fascicles run in a parallel fashion as in the atrionodal bundles. Given that the initial part of the DAVB is often histologically similar to the compact node, some authors only consider the bundle where it becomes surrounded by the tissues of the fibrous body.[11] The term *bundle of His* is commonly used for this structure, named after Wilhelm His Jr., who described it for the first time. In dogs, it is approximately 8–10 mm long and has a width of 1.5–2.0 mm.[27] The presence of two distinct functional strands within the common trunk of the canine His bundle has been described.[27] According to this report, a dorsal strand extends from the dorsal part of the compact node and continues ventrally with the right bundle branch, and a ventral strand extends from the ventral part of the compact node to continue with the left bundle branch. The electrophysiological properties of both strands are similar, with the exception of the conduction velocity which seems to be faster in the ventral strand.[27] Traversing bridges are present between the strands and ensure their activation as a single conducting structure.

The Bundle Branches

The DAVB divides into several branches that supply the Purkinje network of the right and left ventricles (Figures 1.1 and 1.3). A division into right and left bundle branches is common, although variations exist amongst individuals.[7] This division occurs at the level of the upper portion of the interventricular septum beneath the noncoronary and the right aortic leaflets.

The *right bundle branch* courses in the subendocardium of the right side of the interventricular septum.[7] Proximally, it branches from the DAVB approximately 2–3 mm away from the insertion of the septal leaflet of the tricuspid valve and runs as a single chord until it reaches the cranial (anterior) papillary muscle. At this level, it divides into three branches:

1) *Ramification for the conus pulmonalis*: These branches separate from the right bundle at the level of the base of the papillary muscle and spread over the cranial part of the interventricular septum with an irregular pattern to supply the Purkinje fibres in the area of the conus pulmonalis.
2) *Ramification for the free wall*: After the branching for the conus, the right bundle courses around the base of the papillary muscle and proceeds downward, giving

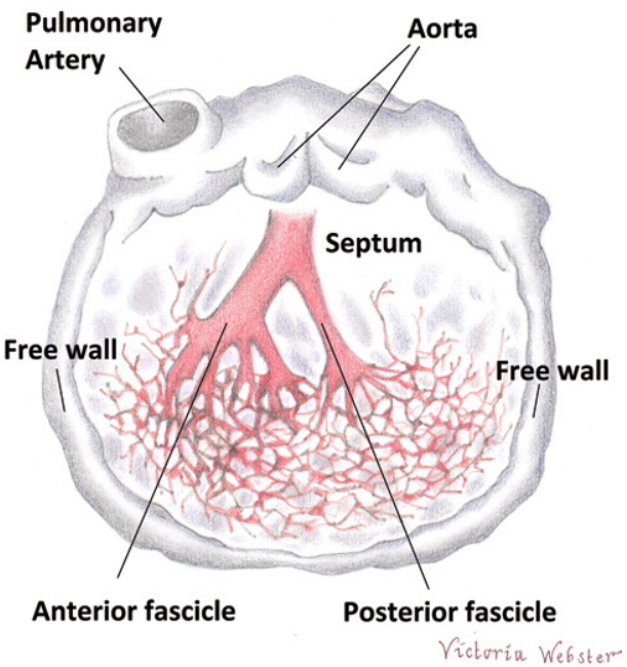

Figure 1.3 The divisions of the left bundle branch. The left bundle branch and its ramifications are illustrated in this picture with the left ventricle open as if cut across its free wall and looking into the septum. The left bundle branch runs in the subendocardium on the left side of the interventricular septum in close proximity to the aortic valve. The initial part (or trunk) is brush-like in shape, approximately 4–7 mm in width and 2–6 mm in length. It ramifies into two main groups of peripheral branches: the *cranial group*, commonly referred to as the anterior fascicle, and the *caudal group* or posterior fascicle. The cranial group splits into a few small branches that run beneath the endocardium for approximately 10–15 mm until they change into bands that project into the ventricular cavity – pseudotendons. Once they reach the base of the cranial (anterior) papillary muscle, they spread to the cranial area of the left ventricle in a mesh pattern. The caudal group gives off a few small branches that run approximately 10–15 mm beneath the endocardium in parallel with each other like a chord until they change into pseudotendons projecting into the ventricular cavity towards the caudal (posterior) papillary muscle. From this point, the Purkinje fibres from the pseudotendons spread over the caudal area of the left ventricle.

off wide and short pseudotendons of approximately 2–3 mm in length and <4 mm in width. These form bridges from the septum to the free wall.

3) *Ramification for the septum*: After the ramifications for the conus and for the free wall, the right bundle gives rise to a few small branches supplying the caudal half of the right side of the interventricular septum.

The *left bundle branch* runs in the subendocardium on the left side of the interventricular septum in close proximity to the aortic valve (Figure 1.3). The initial part (or trunk) of the left bundle is brush-like in shape and approximately 4–7 mm in width and 2–6 mm in length.[7] Its width increases gradually until it ramifies into two main groups of peripheral branches:

1) *Cranial (anterior) group*: The first branch to divide from the trunk splits into a few small branches that run cranially beneath the endocardium for approximately 10–15 mm until they change into bands that project into the ventricular cavity – 'pseudotendons'. Once they reach the base of the cranial (anterior) papillary muscle, they spread to the cranial area of the left ventricle in a mesh pattern.
2) *Caudal (posterior) group*: Another few small branches run approximately 10–15 mm beneath the endocardium in parallel with each other like a chord until they change into pseudotendons, projecting into the ventricular cavity towards the caudal (posterior) papillary muscle. From this point, the Purkinje fibres from the pseudotendons spread over the caudal area of the left ventricle.

Another small subendocardial network of branches from the left bundle has been described between the cranial and caudal groups spreading directly over the septum without giving off pseudotendons – the *intermediate group*.[7]

The terms *anterior* and *posterior fascicles* are often used to describe the cranial and caudal divisions of the left bundle, respectively.

The Purkinje Fibres

The bundle branch subdivisions give rise to numerous small branches that spread all over the subendocardium of both ventricles.[7] These branches are composed of Purkinje cells and form a network connecting the conduction system to the ventricular myocardium. They are more abundant over the base of the papillary muscles and apical regions of the heart. A similar density of Purkinje fibres has been reported in the free wall of both ventricles, but it is higher in the left side of the interventricular septum due to the existence of the intermediate group. As a consequence, the peripheral ramifications are denser in the left ventricle, which makes sense due to its larger dimensions and higher contractile force.

Blood Supply

Sinus Node

The canine SA artery has been reported to derive in most instances (90%) from the distal right atrial branch, a terminal branch of the right coronary artery, and less commonly from a branch of the left coronary artery.[1,28–30] However, other reports showed that the blood supply to the sinus node was instead derived from branches of the left circumflex coronary artery either alone or in combination with distal branches of the right coronary artery.[31,32] This highlights the high

degree of variation possible in this species. The venous return occurs via tiny valveless veins – *Thebesian veins* – that are present in the endocardium and empty directly into the right atrium.

The blood supply of the feline SA also shows a high degree of variation. In most instances, the supply was seen to originate from collaterals of the right circumflex or right coronary arteries, and less frequently from the proximal left atrial branch originating from the left coronary artery.[33]

Atrioventricular Junction

The blood supply to the atrioventricular junction in the dog has been described as originating from two branches from the right coronary artery and one from the left, as well as anastomoses of these vessels in the septum.[34] The DAVB is supplied by the septal artery and the dorsal left artery which are both branches from the left coronary artery. Additionally, perfusion is provided in part by the accessory ventral right atrial branch of the right coronary artery. The venous return occurs via Thebesian veins.

Innervation

The SA and AVN regions of the canine heart are richly innervated by the autonomic nervous system.[35] The SA is especially responsive to parasympathetic stimulation, whereas the AVN is preferentially sensitive to sympathetic tone. The effects of both are discussed in chapter 2.

Sympathetic innervation of both the SA and AVN is provided by sympathetic efferents from the ansae subclaviae via branches of the cervicothoracic ganglia and the middle cervical ganglia.[36] Parasympathetic innervation of the SA is provided by the right vagus, whilst the AVN is innervated by both the right and left vagus nerves. The parasympathetic fibres synapse in ganglia located in the heart and short postsynaptic fibres, then supply the relevant cardiac structures (e.g. the SA and AVN). These ganglia are located in fat pads at the level of the junction between the cranial vena cava and aorta, the caudal vena cava and left atrium and the junction of the right pulmonary vein with the atrium.[37,38] The bundle branches and its ramifications do not seem to be innervated, although autonomic fibres have been identified in close proximity to the subendocardial Purkinje fibres.[39]

References

1 James TN. Anatomy of the sinus node of the dog. Anat Rec. 1962;143:251–265.
2 Nabipour A. Comparative histological structure of the sinus node in mammals. Turk J Vet Anim Sci. 2012;36:463–469.
3 Monfredi O, Dobrzynski H, Mondal T, Boyett MR, Morris GM. The anatomy and physiology of the sinoatrial node: a contemporary review. Pacing Clin Electrophysiol. 2010;33:1392–1406.
4 Kalman JM, *et al.* Radiofrequency catheter modification of sinus pacemaker function guided by intracardiac echocardiography. Circulation. 1995;92:3070–3081.
5 Ghazi SR, Tadjalli M, Baniabbas A. Anatomy of the sinus node of domestic cats (*Felis catus*). J Appl Animal Res. 1998;14:57–64.
6 Opthof T, Dejonge B, Massonpevet M, Jongsma H, Bouman L. Functional and morphological organization of the cat sinoatrial node. J Molec Cell Cardiol. 1986;18:1015–1031.
7 Hara T. Morphological and histochemical studies on the cardiac conduction system of the dog. Archiv Histolog Japon. 1967;28:227–246.
8 Bromberg BI, Hand DE, Schuessler RB, Boineau JP. Primary negativity does not predict dominant pacemaker location: implications for sinoatrial conduction. Am J Physiol. 1995;269:H877–H887.
9 Fedoro VV, *et al.* Structural and functional evidence for discrete exit pathways that connect the canine sinoatrial node and atria. Circ Res. 2009;104:915–923.
10 Holsinger JW, Wallace AG, Sealy WC. The identification and surgical significance of the atrial internodal conduction tracts. Ann Surg. 1968;167:447–453.
11 Ho SY, *et al.* The architecture of the atrioventricular conduction axis in dog compared to man: its significance to ablation of the atrioventricular nodal approaches. J Cardio Electrophysiol. 1995;6:26–39.
12 Wagner ML, Lazzara R, Weiss RM, Hoffman BF. Specialized conducting fibers in the interatrial band. Circ. Res. 1966;18:502–518.
13 Antz M, *et al.* Electrical conduction between the right atrium and the left atrium via the musculature of the coronary sinus. Circulation. 1998;98:1790–1795.
14 Arruda M, *et al.* Dispersion in ventricular repolarization in the human, canine and porcine heart. J Am Coll Cardiol. 2016;120:222–235.
15 Scherlag BJ, Yeh BK, Robinson MJ. Inferior interatrial pathway in the dog. Circ Res. 1972;31:18–35.
16 Sakamoto S, *et al.* Interatrial electrical connections: the precise location and preferential conduction. J Cardio Electrophysiol. 2005;16:1077.
17 Ott P, *et al.* 1014-210 Coronary sinus Os and fossa ovalis ablation: effect on interatrial conduction and inducibility of atrial fibrillation. J Am Coll Cardiol. 2004;43:A105.

18 Meijler FL, Janse MJ. Morphology and electrophysiology of the mammalian atrioventricular node. Physiol Rev. 1988;68:608–647.

19 James TN. Anatomy of the A–V node of the dog. Anat Rec. 1964;148:15–27.

20 Racker DK. The AV junction region of the heart: a comprehensive study correlating gross anatomy and direct three-dimensional analysis. Part II. Morphology and cytoarchitecture. Am J Physiol Heart Circ Physiol. 2004;286:H1853–H1871.

21 Tadjalli M, Ghazi SR, Shahri AB. Anatomy of the atrioventricular node in the heart of cat. J Appl Anim Res. 1999;15:35–40.

22 Racker DK. Atrioventricular node and input pathways: a correlated gross anatomical and histological study of the canine atrioventricular junctional region. Anat Rec. 1989;224:336–354.

23 Moïse NS, Gladuli A, Hemsley SA, Otani NF. 'Zone of avoidance': RR interval distribution in tachograms, histograms, and Poincaré plots of a Boxer dog. J Vet Cardiol. 2010;12:191–196.

24 Antz M, Scherlag BJ, Otomo K, Pitha J. Evidence for multiple atrio-AV nodal inputs in the normal dog heart. J Cardio Electrophysiol. 1998;9:395.

25 Racker DK, Kadish AH. Proximal atrioventricular bundle, atrioventricular node, and distal atrioventricular bundle are distinct anatomic structures with unique histological characteristics and innervation. Circulation. 2000;101:1049–1059.

26 Ho SY, *et al.* The architecture of the atrioventricular conduction axis in dog compared to man: its significance to ablation of the atrioventricular nodal approaches. J Cardio Electrophysiol. 1995;6:26–39.

27 Alanis J, Benitez D. Two preferential conducting pathways within the bundle of His of the dog heart. Jap J Physiol. 1975;371–385. doi:10.2170/jjphysiol.25.371

28 Moore RA. The coronary arteries of the dog. Am Heart J. 1930;5:743–749.

29 Amaral RC, Borelli V, Didio L. The blood supply of the sinu-atrial node of Dobermann dogs. Arch Ital Anat Embriol. 1985;1985.

30 Izumisawa N, Machida N, Kiryu K, Kitayama T. Blood supply of the sinus node artery in beagle dogs. Heart Vess. 1994;9:96.

31 Biasi C, Borelli V, Prazeres RF, Favaron PO. Análise comparativa entre a vascularização arterial ventricular e do nó sinoatrial em corações de cães. Pesq Vet Bras. 2013;33:111–114.

32 Pina JA, Pereira AT, Ferreira SA. [Arterial vascularization of the sino-auricular node of the heart in dogs]. Acta Cardiol. 1975;30:67–77.

33 Biasi, C, Borelli, V, Benedicto HG, Pereira MR. Análise comparativa entre a vascularização ventricular e do nó sinoatrial em gatos. Pesq Vet Bras. 2012;32:78–82.

34 Halpern MH. Blood supply to the atrioventricular system of the dog. Anat Rec. 1955;121:753–762.

35 Randall WC, Ardell JL, O'Toole MF, Wurster RD. Differential autonomic control of SAN and AVN regions of the canine heart: structure and function. Prog Clin Biol Res. 1988;275:15–31.

36 Yuan BX, Ardell JL, Hopkins DA, Losier AM, Armour JA. Gross and microscopic anatomy of the canine intrinsic cardiac nervous system. Anat Rec. 1994;239:75–87.

37 Randall WC, Ardell JL, Wurster RD. Vagal postganglionic innervation of the canine sinoatrial node. J Auton Nerv Syst. 1987;20:13–23.

38 Chiou CW, Eble JN, Zipes DP. Efferent vagal innervation of the canine atria and sinus and atrioventricular nodes: the third fat pad. Circulation. 1997;95:2573–2584.

39 Tcheng KT. Innervation of the dog's heart. Am. Heart J. 1951;41:512–524.

2

Cardiac Electrophysiology

Antonia Mavropoulou

Introduction

As described in chapter 1, the heart possesses a specialised conduction system responsible for the spontaneous generation and transmission of electrical impulses to the whole heart in a specific manner. This is possible due to the presence of different cardiac cells, each with a specific purpose and characteristics. In this chapter, we will discuss the mechanisms that allow the various cardiac cells to generate and transmit electricity. The aim is to cover the basic electrophysiological principles of normal cardiac cell function that are essential to understand how cardiac arrhythmias are generated and how they can be influenced by antiarrhythmic drugs. For the interested reader, a more detailed discussion on cardiac physiology may be found in the textbooks listed under the 'Recommended Reading' section.

Cardiac Cell Types

Cardiac cells may be broadly divided into *pacemaker cells*, *specialised conduction cells* and the *working myocardium*. Throughout this chapter, the differences between each of these cells will become apparent. As the name suggests, the pacemaker cells are responsible for spontaneous generation of electrical impulses. They are prevalently located in the sinus node, although cells in the atrioventricular node (AVN) and His–Purkinje are also capable of performing this task.[1,2] The specialised conduction cells are responsible for rapid (e.g. Purkinje cells) or slow (e.g. AVN) propagation of the electrical impulse that ultimately reaches the working myocardial cells, triggering muscle contraction.

The Cardiac Action Potential

The ability of cells to generate and propagate electrical impulses is linked to the presence and movement of particles (ions or electrolytes) with positive or negative charges between both sides of the cell membrane. Mammalian cells are rich in potassium (K^+ = 150 mmol/L) and magnesium (Mg^{2+} = 12 mmol/L) and are bathed by fluid in the extracellular space that is rich in sodium (Na^+ = 140 mmol/L), calcium (Ca^{2+} = 1 mmol/L), chloride (Cl^- = 110 mmol/L) and bicarbonate (HCO_3^- = 30 mmol/L).[3] If these ions are allowed to move across the cell membrane, they will flow towards the less concentrated area and by doing so will create differences in electrical potential. This flow depends largely on the presence of ion channels, exchangers or pumps in the cell membrane. The various ionic currents across the membrane influence the resting membrane potential (RMP) and the cardiac action potential, as described in the remainder of this section.

Resting Membrane Potential

In the resting state, the inside of the cell is negatively charged, in contrast to the outside in which positive charges prevail. This is mainly due to different concentrations of Na^+ and K^+ molecules on both sides of the cell membrane. As mentioned in the last paragraph, the cell interior is rich in K^+ and the extracellular space is rich in Na^+. Numerous sodium–potassium pumps in the cell membrane constantly remove sodium from the cell (three Na^+ molecules) in exchange for potassium (two K^+ molecules), and this accounts for the accumulation of K^+ in the cell and of Na^+ in the extracellular space. It is apparent from this exchange that more positive charges leave the cell than enter it, leaving the inside of the cell with a deficit of positive charges. Additionally, the cell membrane is semipermeable to K^+, thereby allowing it to leak back into the extracellular space along its concentration gradient, causing an even greater loss of positive charges. By contrast, inward movement of Na^+ occurs to a much lesser extent, as the cell membrane is less permeable to Na^+ in comparison to K^+. Ultimately, these mechanisms are responsible for an imbalance of positive charges on both sides of the cell membrane, accounting for cell polarisation. The RMP of the various cardiac cells varies from –50 to –95 mV (Table 2.1).

Guide to Canine and Feline Electrocardiography, First Edition. Ruth Willis, Pedro Oliveira and Antonia Mavropoulou.

Companion website: www.wiley.com/go/willis/electrocardiography

Table 2.1 Properties of membrane potentials in canine heart

	Sinus node cell	Atrial cardiomyocyte	Atrioventricular node cell	Purkinje fibre	Ventricular cardiomyocyte
Resting membrane potential (mV)	−56±7 mV[a]	−73 mV[b,c]	−50 to −60 mV[d]	−90 mV[e]	−84.2±2.7 mV[f]
Action potential duration (ms)	100–300 ms[g]	138±18 ms[h] 100–300 ms[g]	100–300 ms[g]	300–500 ms[i]	226.5±11 ms[f]
Propagation velocity	1.2–14 cm/s[h]	80 cm/s[j]	5.6±0.7 cm/s[k] 33–50 mm/s[l]	200–250 cm/s[m]	20–48 cm/s[n]
Fibre diameter (um)	5–10 μm[o]	15–20 μm[o]	7 μm[m]	50 μm[m]	20–33 μm[f]

References

a. Woods WT, Urthaler F, James TN. Spontaneous action potentials of cells in the canine sinus node. Circ Res. 1976;39:76–82.
b. Feng J, Yue L, Wang Z, Nattel S. Ionic mechanisms of regional action potential heterogeneity in the canine right atrium. Circ Res. 1998;83:541–551.
c. Li D, Zhang L, Kneller J, Nattel S. Potential ionic mechanism for repolarization differences between canine right and left atrium. Circ Res. 2001;88:1168–1175.
d. Bartos DC, Grandi E, Ripplinger CM. Ion channels in the heart. Compr Physiol. 2015;5:1423–1464.
e. Gadsby DC, Cranefield PF. Direct measurement of changes in sodium pump current in canine cardiac Purkinje fibers. Proc Natl Acad Sci USA. 1979;76:1783–1787.
f. Tseng GN, Robinson RB, Hoffman BF. Passive properties and membrane currents of canine ventricular myocytes. J Gen Physiol. 1987;90:671–701.
g. Britton OJ, Bueno-Orovio A, Van Ammel K, Lu HR, Towart R, Gallacher DJ, *et al.* Experimentally calibrated population of models predicts and explains intersubject variability in cardiac cellular electrophysiology. Proc Natl Acad Sci USA. 2013;110:E2098–E2105.
h. Fedorov VV, Schuessler RB, Hemphill M, Ambrosi CM, Chang R, Voloshina AS, *et al.* Structural and functional evidence for discrete exit pathways that connect the canine sinoatrial node and atria. Circ Res. 2009;104:915–923.
i. Aslanidi OV, Stewart P, Boyett MR, Zhang H. Optimal velocity and safety of discontinuous conduction through the heterogeneous Purkinje-ventricular junction. Biophys J. 2009;97:20–39.
j. Spach MS, Miller WT3, Dolber PC, Kootsey JM, Sommer JR, Mosher CEJ. The functional role of structural complexities in the propagation of depolarization in the atrium of the dog: cardiac conduction disturbances due to discontinuities of effective axial resistivity. Circ Res. 1982;50:175–191.
k. Woods WT, Sherf L, James TN. Structure and function of specific regions in the canine atrioventricular node. Am J Physiol. 1982;243:H41–H50.
l. Spach MS, Lieberman M, Scott JG, Barr RC, Johnson EA, Kootsey JM. Excitation sequences of the atrial septum and the AV node in isolated hearts of the dog and rabbit. Circ Res. 1971;29:156–172.
m. Meijler FL, Janse MJ. Morphology and electrophysiology of the mammalian atrioventricular node. Physiol Rev. 1988;68:608–647.
n. Linnenbank AC, De Bakker JMT, Coronel R. How to measure propagation velocity in cardiac tissue: a simulation study. Front Physiol. 2014;5:267.
o. Boyett MR, Honjo H, Kodama I. The sinoatrial node, a heterogeneous pacemaker structure. Cardio Res. 2000;47:658–687.

Ion Channels, Exchangers and Pumps

To understand the mechanisms that lead to cell depolarisation, it is important to first highlight the differences between the various types of ion carriers involved and how they work. Ion movement across the cell membrane depends on the presence of ion channels, exchangers or pumps:

Ion channels are pore-forming membrane proteins that allow passage of ions along an electrical or concentration gradient when in the open state.[4] Each channel is guarded by one or more gates that control its opening and closing in response to different triggers. Most ion channels involved in cell depolarisation and repolarisation are *voltage-gated*, which means that they open and close in response to differences in voltage across the membrane. Other triggers include ligands (e.g. acetylcholine) and stretch (which is detected by mechanoreceptors).[5]

Ion pumps move ions continuously against their concentration gradients and use energy (in the form of adenosine triphosphate [ATP]) in the process. They are responsible for maintaining the ion gradients across the cell membrane (e.g. a $3Na^+/2K^+$ pump).[4]

Ion exchangers are similar to pumps but exploit the energy stored in ion gradients rather than ATP hydrolysis to move ions against their concentration gradient. For example, the $3Na^+/1Ca^{2+}$ exchanger removes Ca^{2+} from inside the cell against its concentration gradient by moving Na^+ into the cell along its concentration gradient as its driving force. The excess Na^+ is then removed from the cell in exchange for K^+ by the $3Na^+/2K^+$ pump.[4]

Table 2.2 lists the various ion currents involved in cell depolarisation and correspondent carriers and characteristics.

Table 2.2 Ion currents and correspondent carriers involved in cardiac cell depolarisation and repolarisation

Ion current	Activation kinetics	Influenced by
I_{Na} – Fast inward sodium[5,6]	*Voltage-gated* Activation: −70 to −60 mV <1 ms Overshoot: +20 to +35 mV Inactivation: <1 to 4 ms 100% until <−40 mV	• Increases with β-adrenergic stimulation • Blocked by class 1 anti-arrhythmics • Inhibited by hyperkalaemia
$I_{Ca(T)}$ – Transient calcium current[5,6]	*Voltage-gated* Activation: 10–20 ms SA node: −60 to −50 mV Atria: −50 mV Ventricles: Absent −40 mV in cats with HCM[7] Mean open time: 1–2 ms Inactivation: Rapid	• No change with β-adrenergic stimulation • Blocked by nickel and amiloride
$I_{Ca(L)}$ – Long-lasting calcium current[5,6]	*Voltage-gated* Activation: 10–20 ms SA node: −40 mV Atria: −30 mV Ventricles: −30 to −35 mV Mean open time: <1 ms Inactivation: Slow 100% until <0 mV	• Increases with β-adrenergic stimulation • Blocked by class IV anti-arrhythmics (e.g. verapamil and diltiazem), amlodipine and nifedipine
I_{to1} – Transient outward potassium currents[6] I_{to2} – Transient outward calcium-activated chloride current[6]	*Voltage-gated* Activation: <10 ms Inactivation: Variable and voltage-dependent	• Reduced expression with chronic adrenergic stimulation and angiotensin II
I_{Kur}, I_{Kr}, I_{Ks} – Delayed rectifier potassium currents[6]	*Voltage-gated* Activation: Slow, 100% at −10 mV Inactivation: Slow, deactivated by full repolarisation	• I_{Ks} increases with β-adrenergic stimulation • Blocked by class III anti-arrhythmics (e.g. amiodarone and sotalol)
I_{K1} or I_{Kir} – Inward rectifier potassium currents[5,6]	Above RMP: Outward current Below RMP: Inward current Inactivated with depolarisation	• Modified by ethanol and acetaldehyde[8]
$I_{Na/Ca}$ – Sodium-calcium exchange[5]	$3Na^+$ exchanged with $1Ca^{2+}$ Na^+ out if membrane potential is positive Ca^{2+} out if membrane potential is negative	
$I_{Na/K}$ – Sodium–potassium ATPase pump	$3Na^+$ driven out of cell whilst $2K^+$ are driven in 1 ATP molecule used per cycle	• Inhibited by digoxin
I_{Cl} – Chloride current	Inward flow of chloride	• Increases with β-adrenergic stimulation, shortening action potential
Additional currents (sinus node and atrioventricular node cells)		
I_f – Inward sodium (and potassium) current[5,9]	Activated with hyperpolarisation: −90 to −50 mV Pacemaker cells	• Increases with β-adrenergic stimulation • Blocked by ivabradine
I_{ACh} – Acetylcholine-activated potassium channel[6]	G protein-coupled inward potassium channels activated by acetylcholine Prevalent in sinus and atrioventricular nodes	• Parasympathetic stimulation

ATP, Adenosine triphosphate; HCM, hypertrophic cardiomyopathy; RMP, resting membrane potential; SA, sinoatrial node.

Relevant Aspects of Cardiac Cell Structure and Function

The cardiac muscle is organised as a syncytium of cells that are tightly interlinked by the presence of special junctions between adjacent cells called *intercalated disks* (Figure 2.1).[3] These are composed of specialised structures – *desmosomes* and *fascia adherens* – that form tight junctions, creating a strong mechanical link between each cell. Additionally, another structure is present in the intercalated disks that provides a functional connection between cells; it is called the *nexus* or *gap junction*.[5] Gap junctions allow the passage of ions from the cytoplasm of one cell to the next through aqueous pores, making it possible for the depolarisation wave to be transmitted from cell to cell. For this reason, when one cell becomes depolarised, the impulse is transmitted to all adjacent cells, resulting in a depolarisation wave that sweeps the entire myocardium until all cells become depolarised. The number and position of the intercalated disks influence the direction and velocity of the depolarisation wave. In cardiac muscle, they are more prevalent in the direction of the long axis of myocardial fibres, ensuring that the depolarisation wave is propagated in this direction rather than transversally.[10,11] This arrangement is logical as the myocardial fibres are oriented in specific ways that allow the heart to function effectively as a pump. Conduction in the myocardium is therefore *anisotropic* with a conduction velocity that is faster in the direction of the long axis of the myocardial fibres than it is transversally. This property of myocardial conduction has implications for the genesis of arrhythmias, as given the right conditions (e.g. slower conduction in areas with damaged cells), it may allow re-entry to occur (see chapter 6).[12] There are protective mechanisms to prevent this from happening, such as the fact that gap junctions are able to change their electrical resistance in response to various conditions. For example, with myocardial infarction, there is an increase in intracellular calcium levels in damaged cells that causes the gap junctions with neighbouring cells to close in an attempt to protect them from the effects of the injured cells.[13] Changes in pH also have an effect on gap junctions: acidosis causes an increase in electrical resistance, slowing the rate of propagation of the action potential and possibly leading to conduction delay or block; alkalosis has the opposite effect.[14,15] These are some examples of cardiac cell physiology facts that are relevant to the genesis of cardiac arrhythmias in our patients. This topic will be developed further in chapter 6.

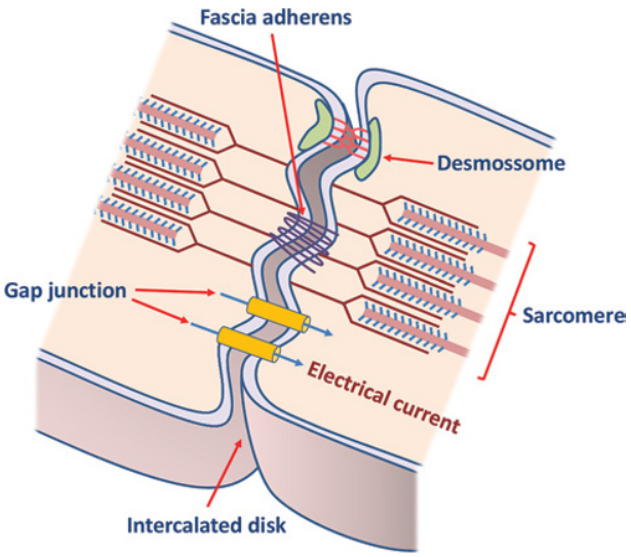

Figure 2.1 The intercalated disk. The intercalated disk is composed of specialised structures – *desmosomes* and *fascia adherens* – that form tight junctions creating a strong mechanical link between cells. The *gap junctions* provide a functional connection between cells that allows passage of ions.

Cell Depolarisation and the Action Potential

Normally, the pacemaker cells in the sinoatrial node are responsible for initiating the depolarisation wave, which is then transmitted to all the cardiac myocytes. There are substantial differences between the depolarisation of conduction system cells (e.g. pacemaker cells, compact node cells and Purkinje cells) and working myocardial cells (e.g. atrial and ventricular). The RMP, and the shape and duration of the action potential, are shown in Figures 2.2 and 2.3.

The action potential in cardiac myocytes is generated by a series of ion movements, as described in the remainder of this section, which focuses on working myocardial and specialised conduction cells. The action potential of the pacemaker cells will be discussed in a separate section later in the chapter.

Stage 0 (rapid depolarisation due to inward flow of Na^+)

In diastole, the RMP of a ventricular cell is close to −85 mV. An action potential triggered in a neighbouring cell causes a slight increase in potential to around −70 to −60 mV, which is the activation threshold for sodium channels, resulting in an inward current of Na^+ (I_{Na}) that effectively causes depolarisation.[10,16] The membrane potential increases to above 0 mV. These channels are characterised by rapid activation (<1 ms) and inactivation (from <1 to 4 ms), which accounts for the very rapid depolarisation and steep upstroke of the action potential. This process is both time- and voltage-dependent, and the Na^+ channels can exist in either of three states: when *activated*, they open; shortly after, they close, becoming *inactivated*; and, once the RMP has been restored, they enter a *resting state* and are ready to open again.

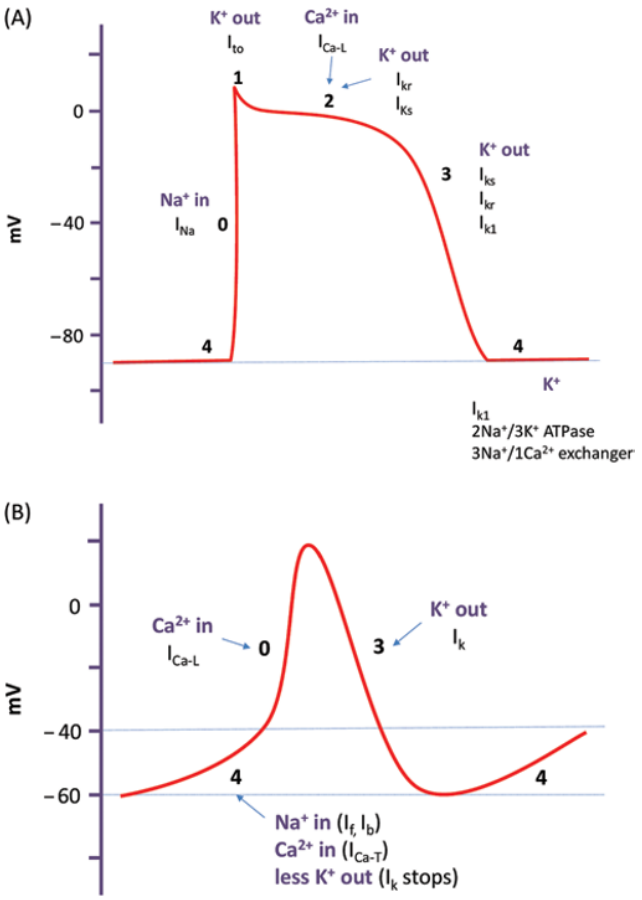

Figure 2.2 Stages of the cardiac action potential and ionic currents. (A) Ventricular myocyte. (B) Pacemaker cell. Note that in ventricular myocytes, the action potential has five stages – 0, 1, 2, 3 and 4 – whereas in pacemaker cells stages 1 and 2 are absent.

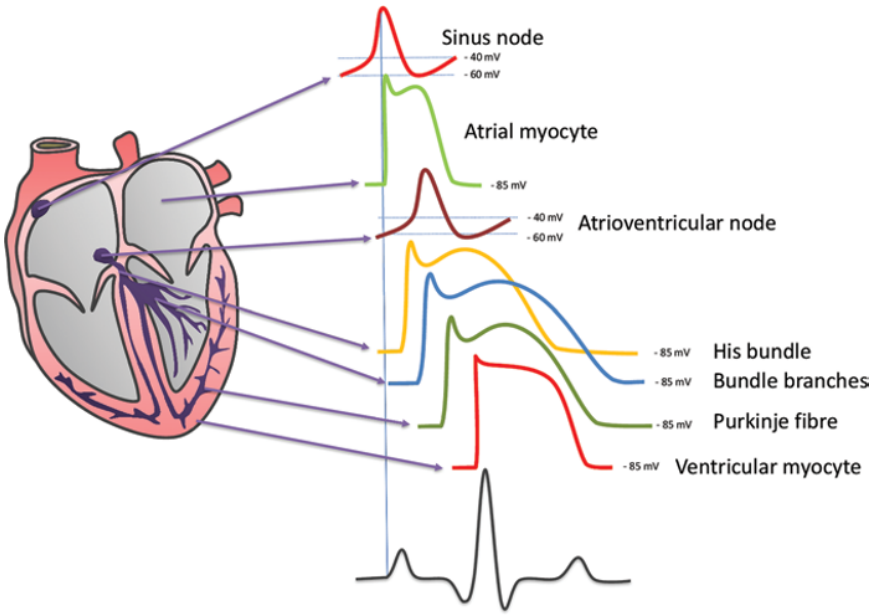

Figure 2.3 The cardiac action potential of the various cardiac cells.

Stage 1 (rapid repolarisation)

With the increase in membrane potential above 0 mV, another type of voltage-gated channels (I_{to}) become activated, allowing the exit of K^+ from the cell.[17,18] At the same time, the Na^+ channels have entered the inactivated state, and the inward Na^+ current has stopped. The combination of these two events leads to a net decrease in membrane potential to approximately 0 mV. This is stage 1 of the action potential. I_{to} channels are present in higher densities in Purkinje cells, atrial cells, epicardial

cells and mid-myocardial ventricular cells in comparison to endocardial ventricular cells, resulting in a more prominent phase 1, as shown in Figure 2.3.[19]

Stage 2 (plateau phase)

During this stage, there is a combination of several ion currents involving a balance between entry of Ca^{2+} in the cell ($I_{Ca\text{-}L}$) and exit of K^+ (I_K and I_{to}).[10,16] During stage 0 of depolarisation, voltage-gated calcium channels (L subtype) become activated when the voltage reaches –35 to –30 mV. They open quickly (<1 ms) but inactivation is slow, accounting for the duration of stage 2 (Figure 2.2). During this period, the inward Ca^{2+} flow will trigger release of Ca^{2+} from the sarcoplasmic reticulum, causing muscle contraction in working myocardial cells. The outward flow of K^+ during this stage is due to activation of several channels, of which the most important are the voltage-gated I_{Kr} (*r* for rapid) and I_{Ks} (*s* for slow) currents. They become fully active during depolarisation when the membrane potential reaches –10 mV, and their function is enhanced with the increased internal calcium levels.[20] The activity of I_{to} channels also has an influence on the duration and amplitude of stage 2.[21] As mentioned in this chapter, they are more prevalent in atrial cells and epi-/mid-myocardial ventricular cells, contributing to a lower plateau phase and shorter action potential (see Figure 2.3).

Stage 3 (repolarisation)

As the L-type calcium channels become inactivated and the $I_{ca\text{-}L}$ current stops, the outward currents of K^+ continue until the RMP is restored once again. In addition to the I_{Kr} and I_{Ks} currents, a background K^+ current (I_{K1} or I_{Kir}) contributes to late phase 3 repolarisation.[10,16] These channels aim to maintain the RMP by allowing the exit of K^+ from the cell if the potential is above the RMP and allowing entry of K^+ into the cell if the membrane potential is below the RMP. During depolarisation, they are briefly shut and open again during the repolarisation stages.

Stage 4 (resting state)

During this stage, the changes that occurred during depolarisation are rectified. The $3Na^+/2K^+$ ATPase pumps and the $3Na^+/1Ca^{2+}$ exchanger work to remove the excess Na^+ and Ca^{2+} from the cell and restore the K^+ levels. It is important to highlight that the ionic movements driving cell depolarisation and repolarisation involve only minute amounts of ions and the cell content of these ions remains virtually unchanged.[16]

Cell Excitability and Refractoriness

The ability to generate an action potential following an electrical impulse of sufficient magnitude represents the *excitability* of the cell. This is proportional to the intensity of the electrical stimulus propagated from cell to cell that is able to trigger depolarisation (stage 0 of the action potential). This will also depend on the RMP and how close it is to the activation threshold which is the membrane potential above which cell depolarisation occurs. If cells are more or less excitable than normal, this will have significant implications on heart rate, conduction velocity and likelihood of arrhythmias.[12,16]

Once depolarisation is triggered, the cell is unable to generate another action potential until repolarisation occurs (from stage 0 until the end of stage 3). The cell becomes *refractory* to additional stimuli during this period because the fast sodium channels become inactivated at membrane potentials above –50 mV. Until the membrane potential falls below this threshold during stage 3 of repolarisation, the cell is incapable of generating another action potential regardless of the intensity of the triggering stimulus. This is the *effective refractory period* (ERP) (Figure 2.4). Whilst the membrane potential is between –50 mV and the resting membrane potential (–85 to –90 mV, which is reached at the end of stage 3), it may be possible for a stimulus of sufficient magnitude to trigger an early depolarisation. The resulting action potential will have a slower stage 0 and will achieve lower voltages which result in a slower conduction velocity, as a proportion of fast sodium channels are still inactive at this stage. This is the *relative refractory period* (RRP). By the end of the RRP, there is a period called the *vulnerable period* in which a stimulus of sufficient intensity may cause a repetitive response. A relevant example would be the triggering of ventricular fibrillation when a premature beat (an ectopic or paced beat) happens to occur during the vulnerable period, which on the electrocardiogram corresponds to the peak of the T wave. The vulnerable period for the atrial myocardium occurs during the descending R wave or during the S wave of the

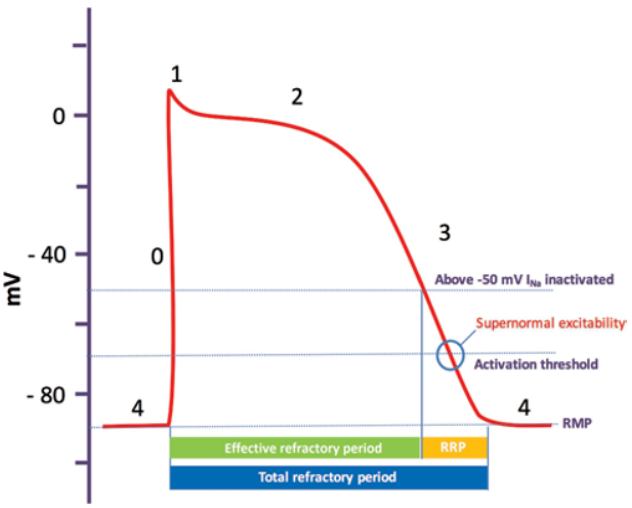

Figure 2.4 Cell refractoriness. RMP, Resting membrane potential; RRP, relative refractory period.